

DEVELOPMENT OF A PROCEDURE FOR EXPERIMENTAL MEASUREMENT OF
SHEAR ENERGY INTENSITY IN TIRE CONTACT PATCH

by

Piyush Mohan Gulve

A thesis submitted to the faculty of
The University of North Carolina at Charlotte
in partial fulfillment of the requirements
for the degree of Master of Science in
Mechanical Engineering

Charlotte

2017

Approved by:

Dr. Peter Tkacik

Dr. Russel Keanini

Dr. Saiful Bari

© 2017
Piyush Mohan Gulve
ALL RIGHTS RESERVED

ABSTRACT

PIYUSH GULVE. Development of A Procedure For Experimental Measurement Of Shear Energy Intensity In Tire Contact Patch. Under the direction of Dr. PETER TKACIK.

Energy dissipated in the contact patch of a rolling tire is related to material abrasion and tire wear. In this study, we calculate the shear energy intensity as the product of the sliding distance and the shear stresses as measured in the tread block sliding deformations and normal load distribution at contact patch for a collection of low profile tires. The objective of the study is to develop a procedure to find pressure distribution in contact patch, tread displacement during rolling and shear energy intensity on low profile tire footprint. Studying shear energy intensity in contact patch of rolling tire will help in better understanding of tire wear.

Shear energy is product of shear stresses and displacement. A new experimental optical method based on Total Internal Reflection was developed to get displacements in a contact patch of a tire. Another new experimental optical method based on Frustrated Total Internal Reflection was developed to get normal stresses in a contact patch of a tire. Load distribution across contact patch of rolling tires was successfully obtained at much lower cost compared to other methods Shear energy intensity distribution across tire contact patch was obtained from these measurements and a coefficient of friction relation.

ACKNOWLEDGEMENTS

I will start by thanking the advisory council and specifically Dr. Peter T. Tkacik for his guidance and enthusiasm during this research. Dr. Tkacik provided insights from the tire industry from his personal and professional experience which further deepened my own interests for career development. I would also like to thank Dr. Russel Keanini and Dr. Saiful Bari for agreeing to be on my thesis defense committee.

A definite thank you to fellow students Surya, Nagarjun, Amol, Jared and Tucker for always willing to lend a hand while navigating through the graduate program. I would like to thank my family for being constant source of motivation.

Lastly I would like to thank the Mechanical Engineering Department for their professionalism, support, and encouragement to be involved with on campus projects pursuant with my own career interests.

TABLE OF CONTENTS

LIST OF FIGURES	VII
CHAPTER 1: INTRODUCTION	1
1.1 ELASTIC BEHAVIOR OF RUBBER	3
1.2. FRICTION	7
1.2.1. FRICTIONAL PROPERTIES OF RUBBER IN SLIDING AND ROLLING	9
1.3. DEFORMATION	11
1.4. STRAIN	12
1.4.1. STRAIN MEASURES	13
1.4.2. INFINITESIMAL STRAIN THEORY	14
1.5. CAMBER ANGLE AND CAMBER THRUST	14
1.5.1. CAMBER ANGLE AND TIRE WEAR	16
1.6. SHEAR ENERGY INTENSITY	18
1.7. ENERGY DISSIPATION IN TIRES	19
1.8. METHODS FOR FINDING ENERGY DISSIPATION IN TIRES	20
1.9 METHOD FOR MEASURING SHEAR ENERGY USING OPTICAL APPROACH DISCUSSED IN THIS THESIS	24
1.9.1. CONCEPT OF TOTAL INTERNAL REFLECTION	24
CHAPTER 2: METHODOLOGY	28
2.1 EXPERIMENTAL SETUP	28
2.2 FOOTPRINTS	31
2.2.1 PROCESS IMPROVEMENT	34

CHAPTER 3: RESULTS	36
3.1 FRICTIONAL FORCE.....	36
3.2 NORMAL LOAD DISTRIBUTION	36
3.3 COEFFICIENT OF FRICTION	39
3.4 TREAD DISPLACEMENT	41
3.5 SHEAR ENERGY INTENSITY.....	46
CHAPTER 4: CONCLUSION	47
CHAPTER 5 FUTURE SCOPE	48
BIBLIOGRAPHY	49

LIST OF FIGURES

Figure 1: Elastic coefficients of rubber for small strains [1]	4
Figure 2 : Oscillatory deformations [1].....	6
Figure 3: Rolling frictional forces [1]	10
Figure 4: Abrasion as a function of pressure [1].....	11
Figure 5: Movement of tread block through the contact patch for free rolling tire [1, 6].....	12
Figure 6: Camber thrust[16].....	15
Figure 7: Camber angle vs lateral force [2]	16
Figure 8: Tread deformation during sliding [3]	17
Figure 9: Shoulder wear due to camber [4].....	17
Figure 10: Tire wear due to camber [4]	18
Figure 11: (a) schematic of tire deformation during rolling. (b) typical signal generated by harvester. (c) Electronic circuit diagram[6]	22
Figure 12: principal of optical measurement of tread deformation [8].....	24
Figure 13: Principle of frustrated total internal reflection [9].....	26
Figure 14: optical tire contact pressure test bench using FTIR [10]	27
Figure 15: modified 4 post lift set up	29
Figure 16: modified 4 post lift set up	29
Figure 17: set up- rear glass	30
Figure 18: set up - front glass with FTIR sheet.....	30
Figure 19: Tire footprint using FTIR at 0^0 camber	31
Figure 20: Tire footprint using FTIR at 0.4^0 camber	32
Figure 21: Tire footprint using FTIR at 1.80 camber	32
Figure 22: Tire footprint using FTIR at 2.3^0 camber	33

Figure 23: Footprint with TIR and white paint	33
Figure 24: Initial footprint image for 2.3^0 camber	34
Figure 25: Footprint images for 2.3^0 camber after method modification.....	35
Figure 26: Gray scale footprint for 0^0 camber	37
Figure 27: gray scale footprint for 0^0 camber after deleting noise.....	37
Figure 28: tire footprint and load distribution in tire contact patch for 6^0 slip angle	38
Figure 295: Coefficient of friction across contact patch.....	40
Figure30: Tire with paint for displacement measurement	42
Figure 31: Tire footprint with sprayed paint at 6^0 slip angle	42
Figure 32: All the particles tracked by dynamic studio red circle shows contact patch at 2.3^0 camber angle	43
Figure 33: 90^0 rotated view and zoomed view of velocity vectors of points on contact patch.....	44
Figure 34: displacement contour across contact patch for 6 degree slip angle in mm.....	45
Figure 35: Shear Stress Intensity across contact patch at 6 degree slip angles	46

CHAPTER 1: INTRODUCTION

Rubber is the main element of tire, which can absorb the vibration and deformation for different loadings; it shows visco-elastic behavior that combines elastic and viscous characteristics. Cord ply networks are embedded in the rubber and preventing excessive deformation for rubber. The bead wire is stiffening material in tire for constraining the deformation of both rubber and cord ply. During high speed driving, tires deform repeatedly and rapidly, and its visco elastic behavior leads to hysteresis. The temperature of a tire rises from the heat generation due to hysteresis effect, which is released from the kinematic deformation of the tire.

Selection of material for tires and tread pattern, while designing the tires is one of the most challenging problems for engineers. Engineers have to combine best features from different purpose built tires such as wet weather grip, high speed performance, all season characteristic etc. Although engineers rely heavily on practical experience when formulating a new pattern, they also need data on aspects as pressure distribution in the contact patch under the tire, size of the contact patch, and the behavior of the various channels under load when they are wet. Acquiring this data is this data is difficult procedure. Size of contact patch can be easily found by applying ink to the tire and then press it against a sheet of paper. But this does not give any estimate of the pressure distribution and it cannot display the behavior of the small tread slits which open under load, because any movement smears the ink. Tire manufacturers need to understand the changes a tire undergoes under various loads and applications to improve handling and response. Also, knowing the void ratio of the tire tread is critical for understanding the

water displacement potential of the tire. The contact pressure distribution data gives important knowledge of tread design and contact pattern to improve performance characteristics.

Footprint studies are important to understand mechanical behavior of tire. As tire rolls on road, pressure in contact patch is unevenly distributed. Variation in pressure distribution in tire contact patch is one of the most significant reasons for uneven tire wear. Bad suspension alignment can be one of the reasons behind uneven pressure distribution. Study of effects of suspension parameters on variation in contact patch pressure distribution is one of the focuses of this study. Study of tread deformation under rolling at different suspension setting and finding energy dissipated at tire road contact are also the objectives. The discussion begins with a description of the apparatus and test method, an explanation of data analysis methodology for footprint load distribution, presentation of the footprint stress and displacement information, and an introduction of the shear stress intensity concept with illustrations of its effectiveness as a tool to guide footprint studies from the perspective of wear.

Footprint or contact patch is the part of tire that is in actual contact with the road surface. It is most commonly used to discuss pneumatic tires. The term is strictly used to describe the portion of the tire tread that touches the road surface. Contact patch is the only connection between the road and the vehicle. The size and shape of the contact patch, as well as the pressure distribution within the contact patch, are important parameters to the ride qualities and handling characteristics of a vehicle. Since the wear characteristics of tires is a highly competitive area between tire manufacturers, a lot of

the research done concerning the contact patch is considered highly proprietary and, therefore, very little is published on the subject. All the work done in this research is based on very limited data available. The contact patch is different when the vehicle is in motion compared to when it is static because of flexible nature of rubber. Generally studies focus on static contact patch as it is so much easier to make observations of the contact patch without the tire in motion. The size, shape, and pressure distribution of contact patch are functions of many things, the most important of which are the load on the tire and the inflation pressure: The larger the load on the tire, the larger the contact patch. The larger the inflation pressure, the smaller the contact patch. These properties are not linearly proportional to the area of the contact. Further, the size of the contact patch cannot be simply calculated as load divided by inflation pressure, and the average contact pressure a tire has with the road surface is not equal to the inflation pressure.

1.1 ELASTIC BEHAVIOR OF RUBBER

Rubber is considered as incompressible in bulk as the modulus of bulk compression for rubber is 2GPa. While tensile modulus of rubber is about 2 to 5 MPa. Compared to tensile value, compression modulus is very high. The Poisson's ratio for rubber is about 0.5. Definitions for elastic properties of rubber are explained in figure 1[1]. Another interesting property of rubber is that rubber block volume remains virtually constant when external forces are applied unless the pressure is very high. The block compresses vertically and expands laterally.

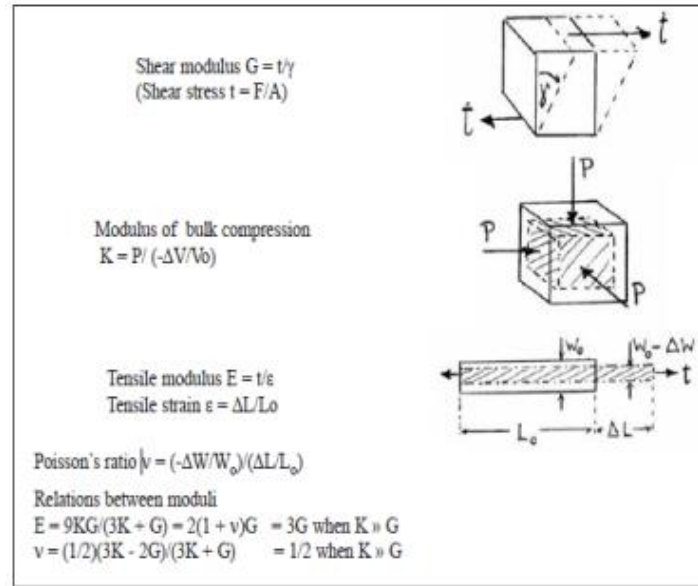


Figure 1: Elastic coefficients of rubber for small strains [1]

1.1.1 ELASTIC BEHAVIOR AT LARGE STRAINS

As mentioned earlier, rubber is highly extensible. So small strain elasticity relationship with moduli G and E to explain the response of rubber to high strains is not sufficient. A term mechanical energy ' W_m ' stored per unit volume by a deformation is used to describe rubber behavior at large strains. W_m can be defined as

$$W_m = (E/\sigma) * J \quad [1]$$

Where J is deformation in terms of stretch ratios λ in principal directions (x, y, z) .

1.1.2 VISCOELASTICITY

Figure 2 shows visco-elastic behavior of rubber compound under repeated oscillations of shear strain (γ). The stress-strain relationship is elliptical. The slope of the line joining points where tangents to ellipse are vertical is called dynamics shear modulus G' (MPa). G' is defined as elastic peak shear stress divided by elastic peak shear strain. The area of ellipse represents energy dissipated in unit volume per cycle of deformation. The dissipated energy is given by

$$U_d = \pi * G'' * \gamma_m^2 \quad [1]$$

Where,

U_d = Energy dissipated

G'' = dynamics shear loss modulus (If deformation is tensile it is denoted by E'')

γ_m = magnitude of shear stress.

γ_m is viscous quantity. The ratio of G''/G' is called $\tan\delta$, phase angle by which strain lags applied stress. If ellipse axes in figure 2 are in vertical or horizontal, value of δ is 90° . $\tan\delta$ is infinite. It indicates the rate of strain is at its max value when applied stress is max. Viscous liquids tend to behave in this manner. When the ellipse diminishes in a straight, δ is 0. $\tan\delta$ is zero. This is behavior of perfect elastic solids. For rubber, values of $\tan\delta$ at room temperature vary from 0.03 to 0.2. Low $\tan\delta$ value rubber act as a highly resilient springy material. While high $\tan\delta$ value rubber compounds have high energy dissipation rates. Generally tread rubber compounds have $\tan\delta$ values of about 0.2.

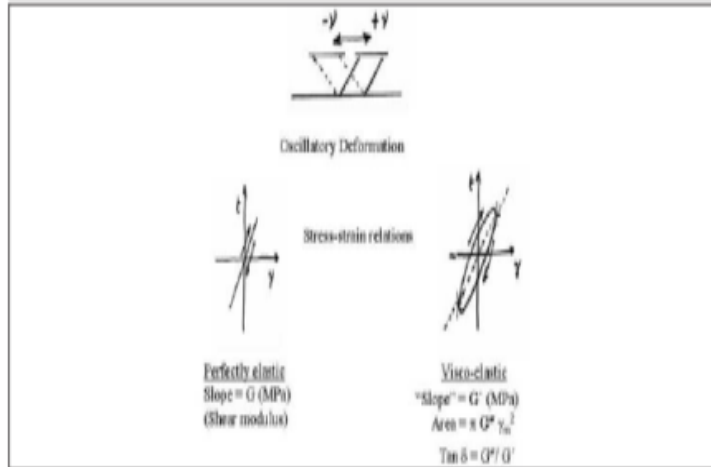


Figure 2 : Oscillatory deformations [1]

$\tan \delta$ is the ratio of viscous property to the elastic property of material. Since it is ratio, it is dimensionless quantity. It is related to oscillatory shear deformation. $\tan \delta$ value is always high in uncured rubber than that of cured state. It represents the processability of uncured rubber compound in uncured state. Higher the value better is processability. It also relates to heat generation due to hysteresis and is inversely proportional to resilience (rebound) of rubber in cured state. Rebound resilience term is used to assess energy dissipation. It is determined by performing drop ball test, also known as rebound test. The test is conducted by dropping rigid ball on a rubber block and measuring rebound, or dropping a rubber ball rigid plate. In both cases the fractional amount of energy returned after impact is

$$R = h_2/h_1,$$

Where,

R is Resilience

h_1 is the height from which ball is dropped

h_2 is the rebound height. If impact is considered as half cycle of oscillation, then

$$\ln R = -\pi \tan \delta$$

This equation is based on assumptions so it is considered as rough approximation. Since resilience can be performed easily, it is commonly used to estimate loss properties.

1.2. FRICTION

Contact mechanics studies the deformation of solids that touch each other at one or more points. It is further divided into compressive and adhesive forces in the direction perpendicular to the interface, and frictional forces in the tangential direction. Frictional contact mechanics is the study of the deformation of bodies in the presence of frictional effects. Frictional contact mechanics is concerned with a large range of different scales. At the macroscopic scale, it is applied for the investigation of the motion of contacting bodies. The bouncing of a rubber ball on a surface depends on the frictional interaction at the contact interface. Here the total force versus indentation and lateral displacement are of main concern. At the intermediate scale, the local stresses, strains and deformations of the contacting bodies in and near the contact area are studied. Application areas of this scale are tire-pavement interaction, railway wheel-rail interaction, roller bearing analysis, etc. At the microscopic and nano-scales, contact mechanics is used to increase our understanding of tribological systems, e.g. investigate the origin of friction, and for the engineering of advanced devices like atomic force microscopes and MEMS devices.

Central in the analysis of frictional contact problems is the understanding that the stresses at the surface of each body are spatially varying. Consequently, the strains and deformations of the bodies are varying with position too. And the motion of particles of the contacting bodies can be different at different locations: in part of the contact patch particles of the opposing bodies may adhere (stick) to each other, whereas in other parts of the contact patch relative movement occurs. This local relative sliding is called micro-slip.

Wear occurs only where power is dissipated, which requires stress and local relative displacement (slip) between the two surfaces. The size and shape of the contact patch itself and of its adhesion and slip areas are generally unknown in advance. If these were known, then the elastic fields in the two bodies could be solved independently from each other and the problem would not be a contact problem anymore. Three different components can be distinguished in a contact problem. The deformation of the separate bodies in reaction to loads applied on their surfaces. This is the subject of general continuum mechanics. It depends largely on the geometry of the bodies and on their constitutive material behavior. Second is the overall motion of the bodies relative to each other, e.g. the bodies can be at rest or approaching each other quickly, and can be shifted or rotated over each other. These overall motions are generally studied in classical mechanics. Third, there are the processes at the contact interface: compression and adhesion in the direction perpendicular to the interface, and friction and micro-slip in the tangential directions.

The last aspect is the primary concern of contact mechanics. It is described in terms of

so-called “contact conditions”. For the direction perpendicular to the interface, the normal contact problem, adhesion effects are usually small (at larger spatial scales).

1.2.1. FRICTIONAL PROPERTIES OF RUBBER IN SLIDING AND ROLLING

Conventionally, the resistance to frictional sliding of one surface on another is given as

$$\mu = F/N$$

Where, μ is frictional coefficient, F is frictional force and N is normal force. But for soft rubber sliding on a smooth surface, the frictional force is constant and independent of the load N , or pressure P . The reason may be complete contact is achieved between soft rubber and a smooth surface at quite small loads. Also further increases in normal load cannot increase the degree of interaction between the two materials and so the frictional force no longer increases. However, for harder rubber compounds sliding against a rough surface, frictional force increases proportional to the applied load or pressure. The contact between two surfaces is incomplete, for harder rubber compounds such as those used in tire treads. An increase in pressure creates a larger true area of contact and hence a larger frictional force.

In case of rolling friction contact, Consider the pressure distribution set up in the contact zone when a rubber cylinder rolls on a rigid surface. For dissipative materials the center of pressure will be located towards leading edge instead of at the center of contact. This is because stresses set up on loading of dissipative materials are higher than those set up while unloading. This is feature of dissipative and visco-elastic materials in

particular. [1] Moreover, the displacement of the center of pressure, and hence the torque required to maintain the motion, will depend on speed and temperature. In figure 3 M represents torque, z is displacement and N is normal load.

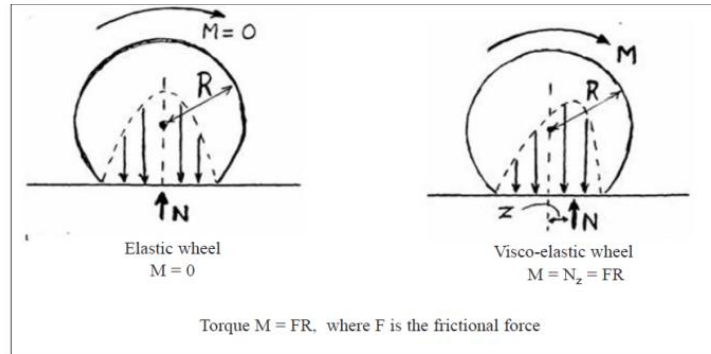


Figure 3: Rolling frictional forces [1]

Abrasion or wear occurs whenever two bodies slide against each other under friction. Material is transferred from one body to the other and this process can go in both directions. Wear is therefore associated with friction. Friction is present in every aspect of life and indeed life would not be possible without it. Although it is a dissipative process in which mechanical energy is turned into heat, high friction is often useful, and even essential, and the resulting wear has to be tolerated. Research tries to find ways to retain high friction while minimizing wear.

Figure 4 [1] shows the results of study by Grosch for abrasion loss of a BR tread compound on four surfaces of different sharpness, as a function of the pressure using logarithmic scales for both axes.

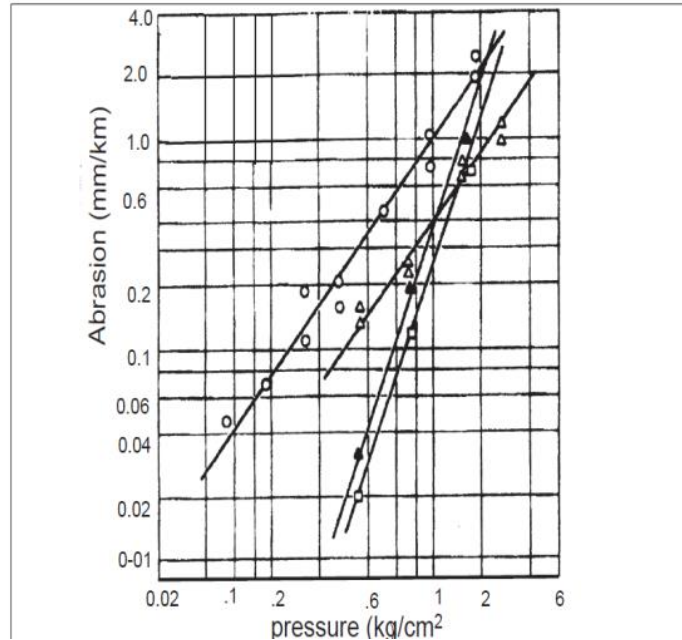


Figure 4: Abrasion as a function of pressure [1]

1.3. DEFORMATION

Deformation is defined in continuum mechanics as the transformation of a body from a reference configuration to a current configuration. A configuration is a set containing the positions of all particles of the body. A deformation may be caused by external loads, body forces such as gravity or electromagnetic forces or changes in temperature, moisture content, or chemical reactions, etc. Strain is a description of deformation in terms of relative displacement of particles in the body that excludes rigid-body motion. In a continuous body, a deformation field results from a stress field induced by applied forces or is due to changes in the temperature field inside the body. The relation between stresses and induced strains is expressed by constitutive equations, e.g., Hooke's law for linear elastic materials. Deformations which are recovered after the stress field has been removed are called elastic deformations. In elastic deformations, the continuum

completely recovers its original configuration. On the other hand, irreversible deformations remain even after stresses have been removed. One type of irreversible deformation is plastic deformation, which occurs in material bodies after stresses have attained a certain threshold value known as the elastic limit or yield stress, and are the result of slip, or dislocation mechanisms at the atomic level. Another type of irreversible deformation is viscous deformation, which is the irreversible part of viscoelastic deformation.

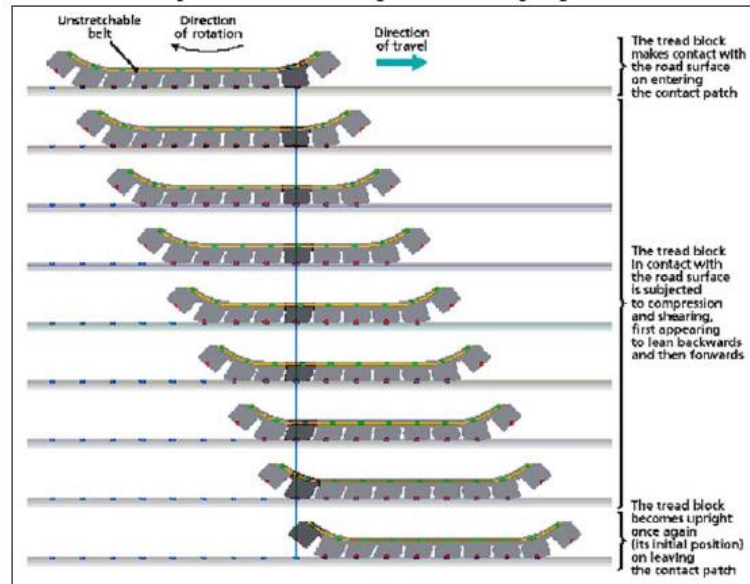


Figure 5: Movement of tread block through the contact patch for free rolling tire [1, 6]

1.4. STRAIN

Strain is a measure of deformation representing the displacement between particles in the body relative to a reference length. A general deformation of a body can be expressed in the form $x = F(X)$ where X is the reference position of material points in the body. Such a

measure does not distinguish between rigid body motions (translations and rotations) and changes in shape (and size) of the body. A deformation has units of length. Strain energy is stored within an elastic solid when the solid is deformed under load. In the absence of energy losses, such as from friction, damping or yielding, the strain energy is equal to the work done on the solid by external loads. Strain energy is a type of potential energy.

1.4.1. STRAIN MEASURES

Depending on the amount of strain, or local deformation, the analysis of deformation is subdivided into three deformation theories:

Finite strain theory, also called large strain theory, large deformation theory, deals with deformations in which both rotations and strains are arbitrarily large. In this case, the undeformed and deformed configurations of the continuum are significantly different and a clear distinction has to be made between them. This is commonly the case with elastomers, plastically-deforming materials and other fluids and biological soft tissue.

Infinitesimal strain theory, also called small strain theory, small deformation theory, small displacement theory, or small displacement-gradient theory where strains and rotations are both small. In this case, the undeformed and deformed configurations of the body can be assumed identical. The infinitesimal strain theory is used in the analysis of deformations of materials exhibiting elastic behavior, such as materials found in mechanical and civil engineering applications, e.g. concrete and steel.

1.4.2. INFINITESIMAL STRAIN THEORY

In continuum mechanics, the infinitesimal strain theory is a mathematical approach to the description of the deformation of a solid body in which the displacements of the material particles are assumed to be much smaller (indeed, infinitesimally smaller) than any relevant dimension of the body; so that its geometry and the constitutive properties of the material (such as density and stiffness) at each point of space can be assumed to be unchanged by the deformation.

With this assumption, the equations of continuum mechanics are considerably simplified. This approach may also be called small deformation theory, small displacement theory, or small displacement-gradient theory. It is contrasted with the finite strain theory where the opposite assumption is made.

The infinitesimal strain theory is commonly adopted in civil and mechanical engineering for the stress analysis of structures built from relatively stiff elastic materials like concrete and steel, since a common goal in the design of such structures is to minimize their deformation under typical loads.

1.5. CAMBER ANGLE AND CAMBER THRUST

Camber thrust and camber force are terms used to describe the force generated perpendicular to the direction of travel of a rolling tire due to its camber angle and finite contact patch. Camber thrust is generated when a point on the outer surface of a leaned and rotating tire, that would normally follow a path that is elliptical when projected onto the ground, is forced to follow a straight path while coming in contact with the ground,

due to friction. This deviation towards the direction of the lean causes a deformation in the tire tread and carcass that is transmitted to the vehicle as a force in the direction of the lean.

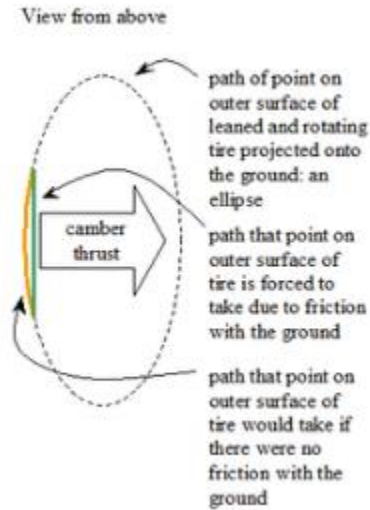


Figure 6: Camber thrust[16]

Camber thrust is approximately linearly proportional to camber angle for small angles, it reaches its steady-state value nearly instantaneously after a change in camber angle, and so does not have an associated relaxation length. Bias-ply tires have been found to generate more camber thrust than radial tires. Camber stiffness is a parameter used to describe the camber thrust generated by a tire and it is influenced by inflation pressure and normal load. The net camber thrust is usually in front of the center of the wheel and so generates a camber torque, twisting torque, or twisting moment. The orientation of this torque is such that it tends to steer a tire towards the direction that it is leaned. An alternate explanation for this torque is that the two sides of the contact patch are at

different radii from the axle and so would travel forward at different rates unless constrained by friction with the pavement.

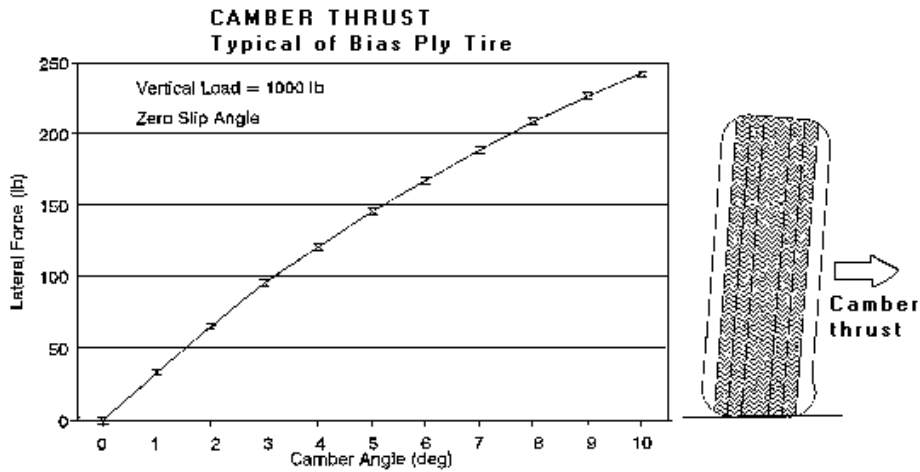


Figure 7: Camber angle vs lateral force [2]

1.5.1. CAMBER ANGLE AND TIRE WEAR

Any angle other than zero camber will cause wear and tear on the tire when driving in a straight line. This is because the tire is still angled, creating an un-uniform contact patch. For this reason, vehicle design engineers have to make a compromise between the camber's benefits when turning, and the damage it will cause to the TIRE when going straight.

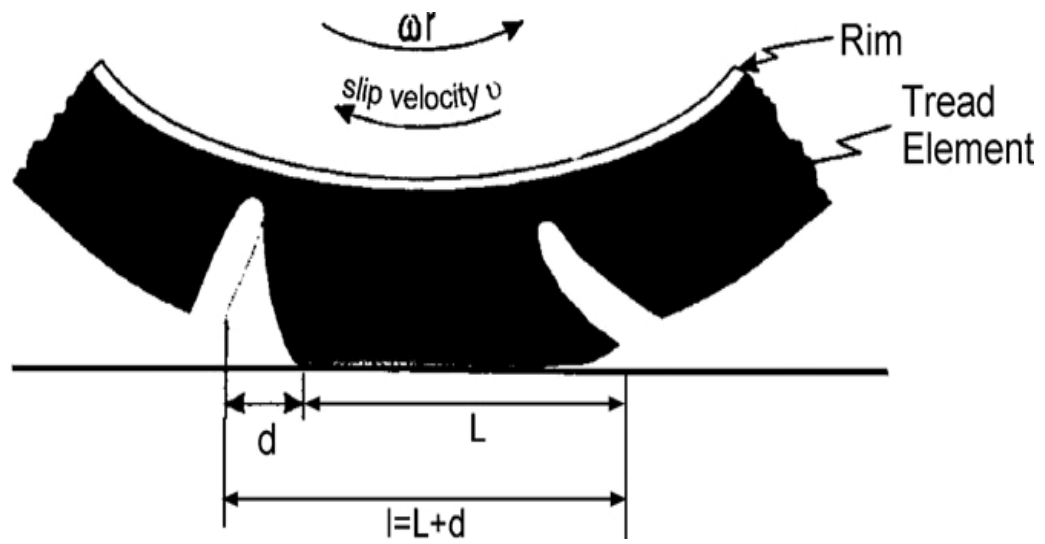


Figure 8: Tread deformation during sliding [3]



Figure 9: Shoulder wear due to camber [4]



Figure 10: Tire wear due to camber [4]

1.6. SHEAR ENERGY INTENSITY

Finding shear energy intensity from all the collected data is a real problem of this project.

The shear energy intensity is defined as the total energy crossing the boundary between the tire and the road due to only shear stresses and displacements reported on a per-unit area basis [12]. For each pass of tire, the work done at contact patch can be calculated from equation [12]

$$W_{ij} = \oint_S \bar{F}_{ij} \cdot d\bar{S}_{ij}$$

Where,

$W_{i,j}$ - Shear work at point i,j

F_{ij} – Footprint force at point ij on tread surface

i,j – position index with respect to tread surface

dS – differential footprint displacement vector

Differential shear work varies point to point. It can be approximated as described from equation below

$$dW_{ij,k} = 0.5[(Fx_{ij,k} + Fx_{ij,k-1})(u_{ij,k} - u_{ij,k-1})] \\ + 0.5[(Fy_{ij,k} + Fy_{ij,k-1})(v_{ij,k} - v_{ij,k-1})]$$

Shear work has a sign. The road does work on the tread and the tread also works on the road. From the standpoint of the tread material at the interface between the tire and road, the sign is not important. But the total amount of shear energy that is generated at the interface per unit area of the tread surface during passage through contact is important. This energy per unit area is the shear energy intensity.

1.7. ENERGY DISSIPATION IN TIRES

Dynamic mechanical testing and material testing have been conducted in relation to the evaluation of hysteresis (H) and total strain energy (U), respectively. Hysteresis loss energy is given as $(H \times U)$ and considered to relate directly to heat generation rate.

Temperature rise is assumed to be due to the energy dissipation from periodic deformation. This dissipation of energy may be equated to be the primary heat generation source. Hysteresis energy loss is used as a bridge to link the strain energy density to the

heat source in rolling tires; temperature distribution of rolling tires may be obtained by the steady-state thermal analysis.

Hysteresis (H) is one of the most commonly used constants and defined as the energy loss part divided by the total energy in kinematic deformation cycle:

$$H = \text{Loss part} / \text{Total part} [5]$$

Various methods can be used to calculate Vertical stiffness of tire using strain energy.

Structural damage detection method using modal strain energy method can also be used to analyse structural damage of tire compounds. Measurement of strain energy in real time is concept of smart future tires, which will help improving tire performance.

1.8. METHODS FOR FINDING ENERGY DISSIPATION IN TIRES

1.8.1. STRAIN ENERGY MEASUREMENT USING PIEZOELECTRIC POLYMER COMPOSITES

Development of wireless autonomous sensors is a rapidly developing field for monitoring systems ranging from distributed sensing to industrial structural health monitoring. The success of this field depends on many factors such as low power data acquisition and processing and efficient energy management energy supply to sensors. There are many different ways of powering these sensors, such as photovoltaic, thermoelectric and vibration based power sources. The most appropriate converter depends on the power source present in the local environment

Direct energy harvesting devices are essentially foil-type devices with limited thickness, which are attached directly to the host structure. The energy harvester will follow the deformations of the host structure, thereby harvesting energy from the environment. Advantages of this type of energy harvesting include higher bandwidth, ease of manufacturing and assembly and ease of structure integration. Electromagnetic and piezoelectric power generators are tried before to build energy harvesters inside automotive tires but there are limitations for this type of methods. The electromagnetic (inductive) systems are relatively bulky, generate low voltages or require an external source outside the tire, adding to system complexity and cost. Concepts based on piezoelectric materials are also been considered based on bender type energy harvesters using ceramic lead zirconate titanate (PZT) in a mass–spring system. This brittle ceramic is not practical to use in automobile tires unless elaborate stress transfer mechanisms are employed, requiring very tight manufacturing tolerances in order to function properly. Moreover, PZT ceramics lose their stiffness and piezoelectricity at high strain levels due to mechanical depoling, which could affect the output of these types of energy harvesters during their lifetime.

When a piezoelectric material is attached to the inside of the tire, the corresponding strains due to the tire–road contact are directly transferred to the energy harvester, which will generate charge as a result of this deformation

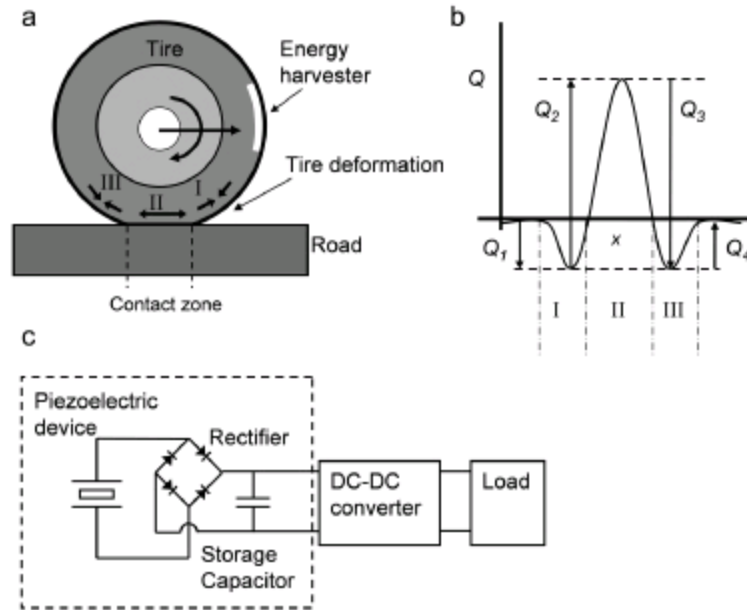


Figure 11: (a) schematic of tire deformation during rolling. (b) typical signal generated by harvester. (c) Electronic circuit diagram[6]

Figure 11 shows experimental set up and schematics of energy harvester. Part (a) shows schematic of the deformation that an automobile tire experiences during a revolution. An energy harvesting material which is adhered to the inner liner of the tire will experience compressive stress before and after the contact zone (I and III), and tensile stress in the contact zone (II). Part brepresents typical charge signal that is generated by the energy harvester in a rolling tire. Part c describes basic electronic circuit for one stage power management in piezoelectric based energy harvesters

LIMITATIONS- An automobile tire fitted with sensors, signal conditioning electronics and a data transmitter. As amount of electronics in automobile tires increase, as will the data rate, increasing power consumption of the tire electronics. This means battery powered modules will not achieve a sufficient lifetime [6]

1.8.2. OPTICAL MEASUREMENT OF TREAD DEFORMATION

Y. Xiong and et all [7] performed developed technique for optical measurement of tread deformation of tires. Their set up included a optical tire sensor platform that included two laser triangular sensors, a slip ring package with an angular sensor, and a data acquisition and processing system was proposed. One laser sensor was capsulated and assembled on a steel passenger car rim to measure the distance L1. The sampling frequency of the sensor was 3 kHz. In addition, another laser sensor (Keyence LK-H150) was selected for the loaded radius L2 measurement. This sensor was fixed to a rigid mechanical support attached to the stator of the slip ring. The sensor has a small laser spot diameter ($\phi = 120\mu\text{m}$) and an ultra-high sampling frequency (392 kHz), because of the requirement to capture the micro-roughness of the road surface at normal driving velocities. The slip ring package (Michigan Scientific SR10AW/T512) is able not only to transmit signals in multiple channels from a rotating TIRE but also to measure the circumferential position of Laser 1. The data acquisition system was implemented through the NI DAQ system and the post-processing algorithm was developed in Matlab. The sampling frequency of the DAQ system was selected to be 10 kHz.

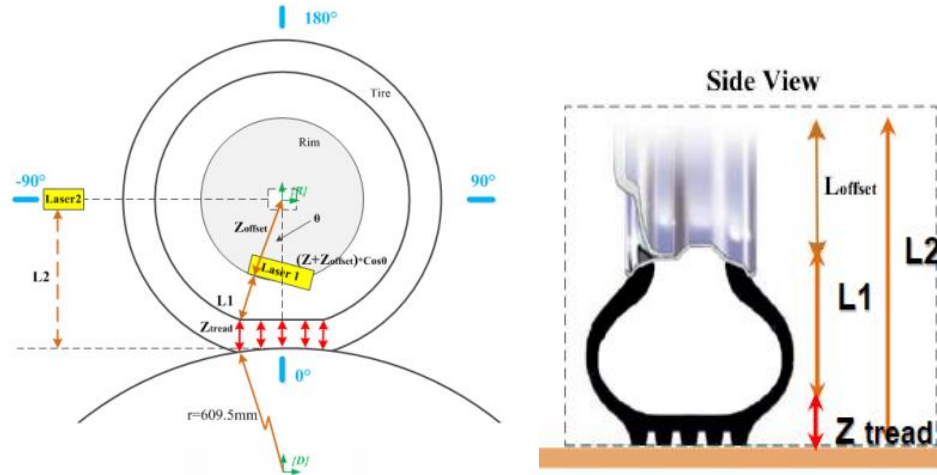


Figure 12: principal of optical measurement of tread deformation [8]

Compressed tread thickness can be found using formula

$$Z_{tread} = L_2 - (L_1 + L_{offset}) * \cos \theta$$

1.9 METHOD FOR MEASURING SHEAR ENERGY USING OPTICAL APPROACH

DISCUSSED IN THIS THESIS

1.9.1. CONCEPT OF TOTAL INTERNAL REFLECTION

Total internal reflection, in physics is defined as a complete reflection of a ray of light within a medium such as water or glass from the surrounding surfaces back into the medium. The phenomenon occurs if the angle of incidence is greater than a certain limiting angle, called the critical angle. In general, total internal reflection takes place at the boundary between two transparent media when a ray of light in a medium of higher

index of refraction approaches the other medium at an angle of incidence greater than the critical angle.

The critical angle is the angle of incidence for which the angle of refraction is 90° . The angle of incidence is measured with respect to the normal at the refractive boundary.

Consider a light ray passing from glass into air. The light emanating from the interface is bent towards the glass. When the incident angle is increased sufficiently, the transmitted angle (in air) reaches 90 degrees. It is at this point no light is transmitted into air.

The phenomenon of frustrated total internal reflection is used to get tire footprints. When light approaches an interface between two optical media of different refractive indices, then in order for it to pass from the dense medium its angle of incidence must be less than some critical angle. When the critical angle is exceeded, the light is totally internally reflected back into the dense medium. However, there is still an electric disturbance in the low density medium within a few wavelengths of the interface, even though all the light energy has been reflected. If now a third medium is brought close to the interface, with a high optical density, then the light will be partially transmitted across the gap, and so the total internal reflection is frustrated.

Figure13 [9] shows how this phenomenon is used in the device described. Light is shone into the edges of a flat glass plate in air, and is totally internally reflected back and forth across the plate, except where a third medium, in this case a textured thin sheet of table cloth, touches the interface. At these points of contact the light escapes from the glass and illuminates the white colored thin sheet so that an observer below the glass plate sees a bright point for every contact. If now a tire is loaded into the thin sheet then the tiny

raised dimples on the sheet are pressed against the glass by varying amounts. Over a limited range of pressures the deformation of the sheet dimples is such that the brightness at any region, observed from below, is proportional to the pressure being applied at that region. Hence, in principle, the phenomenon can be used to give a direct display of a pressure distribution in a tire contact patch by transforming it to a brightness distribution.

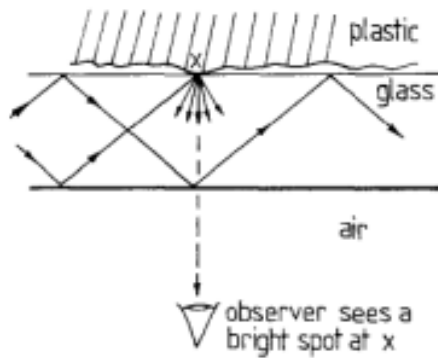


Figure 13: Principle of frustrated total internal reflection [9]

Before the system can be put into practice, two aspects must be studied in relation to the special requirements of a tire investigation apparatus. Firstly, the size of the test surface needs to be chosen, and the area over which an acceptably uniform light distribution can be achieved needs to be established. Secondly, the precise kind of texture and composition for the plastic interface needs to be found so that the relationship between brightness and pressure is linear within the working range of contact pressures found under tires.

The key to the realization of the full potential of this apparatus, however, is the fact that the brightness of the monochrome video picture is a measure of the pressure at any point

in the contact. Hence, if the brightness can be quantified, then a detailed pressure map of the contact patch may be drawn.

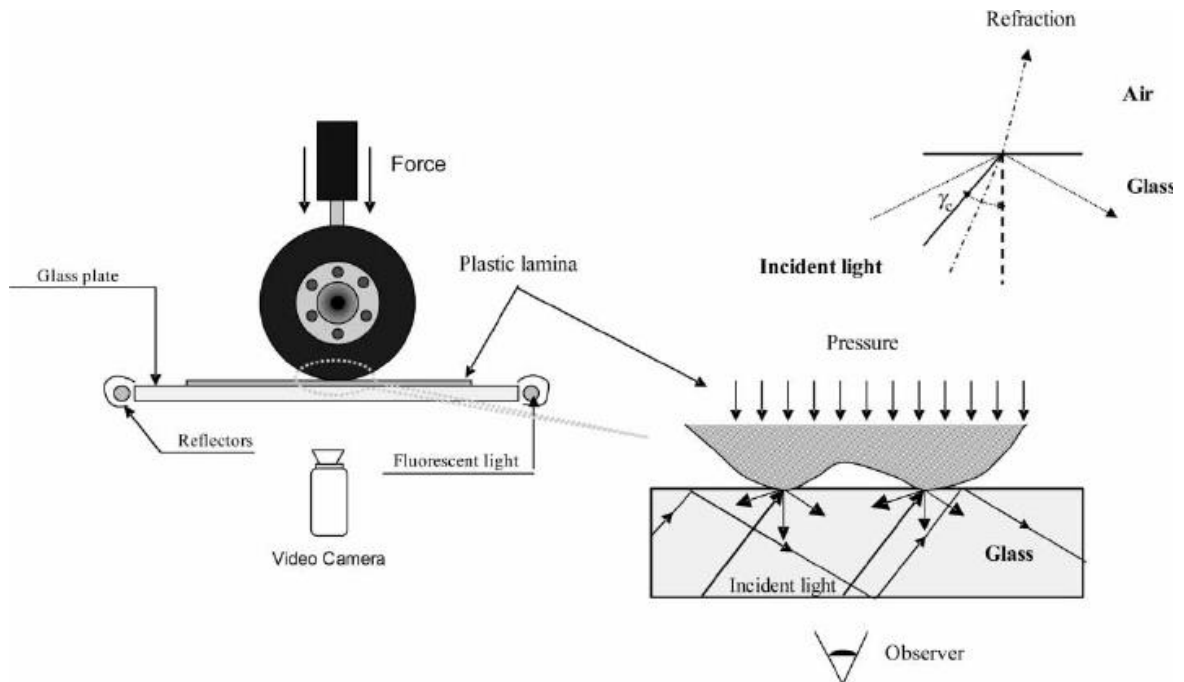


Figure 14: optical tire contact pressure test bench using FTIR [10]

CHAPTER 2: METHODOLOGY

As discussed earlier shear energy intensity in tire contact patch is function of shear forces acting between tire and road surface and tread displacement. To calculate shear energy intensity we must have these quantities. This chapter discusses the optical approach used to find frictional force and tread displacement.

2.1 EXPERIMENTAL SETUP

A four post lift was modified to perform the experiment. Ramp was cut to make place for two glass plates. Both front and rear tires of a car can be driven on a set up. Plates were shone with light from sides using LED lights to use total internal reflection phenomenon. Digital camera with multi point focus capability, 4k resolution was used. Camera was placed under the glass plate to get tire footprints of rolling tire. Tire footprints were recorded with and without FTIR technique. As discussed earlier a thin cloth was used to get FTIR images. FTIR technique is used to obtain pressure distribution in footprint while tread displacement can be observed with footprints without FTIR. tire was painted with white dots for displacement measurements. As tire rolls, displacement of each white dot is measured. Both load and displacement techniques are discussed later in separate chapters. Porsche 911 tires (front- P205/50 R17, rear 255/40R17) were used for this study.



Figure 15: modified 4 post lift set up



Figure 16: modified 4 post lift set up



Figure 17: set up- rear glass



Figure 18: set up - front glass with FTIR sheet

The inflation pressure was 35 psi. Inclination angles from 0° to 2.5° are duplicated for the straight-ahead rolling, and peak right turn conditions. Each tire variant is measured for

friction energy distribution on the tread elements. Toe angle was changed from 0° to 6° . Supporting frame was created to support glass in case of sliding. All suspension settings were measured using Hunter DSP machine.

Experiment was carried with tires mounted on vehicle. Vehicle was rolled on glass at slow speed to observe tread displacement. Tire rolling motion was recorded in slow motion videos. Motion of left front tire was observed in this case.

2.2 FOOTPRINTS



Figure 19: Tire footprint using FTIR at 0° camber



Figure 20: Tire footprint using FTIR at 0.4° camber



Figure 21: Tire footprint using FTIR at 1.80° camber



Figure 22: Tire footprint using FTIR at 2.3° camber

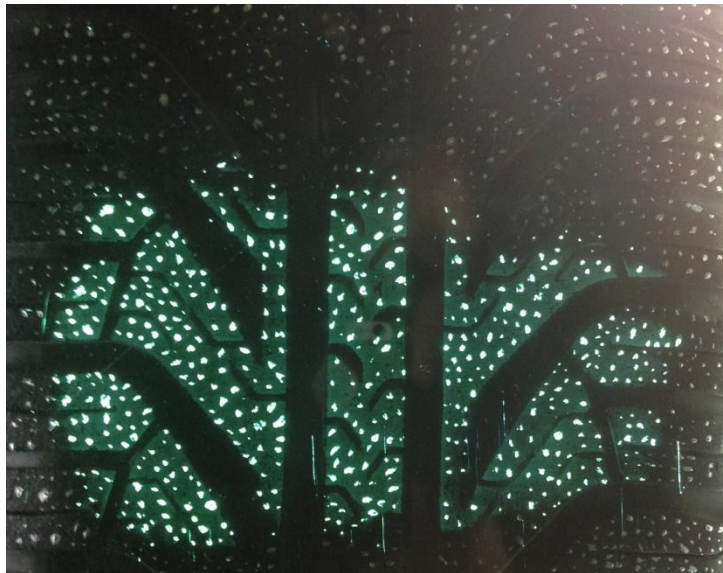


Figure 23: Footprint with TIR and white paint

2.2.1 PROCESS IMPROVEMENT

The FTIR technique uses a material to create frustration in total internal reflection. In this case a thin cloth was used for this purpose. Images obtained were of good quality and were representing expected load distribution across footprint. But to further improve image quality and get sharper images we tried different cloths with various pattern and thickness. Every material gave little variation in image qualities. After many trials we came down to final selection of one which gave sharpest possible pattern. Also different light sources were used to transmit light across glass plate. Halogen lamps of different power, neon lights, LED strips with different number of small bulbs were tested. Camera focal lengths and pixels were varied for better resolution images.



Figure 24: Initial footprint image for 2.3⁰ camber



Figure 25: Footprint images for 2.3° camber after method modification

It can be observed from tire footprints that as camber angle is varied from positive 0 to 2.3° , tire footprint size is reduced dramatically. Tire loses contact with road as camber increases though contact on outer edge is more. It also indicates that increasing camber above 2.5° - 3° doesn't make much sense road vehicles.

If the track is smooth the abrasive loss may be so small that it eludes normal measurement, although the frictional force may be very high, while on rough sharp surfaces the abrasive loss may be pronounced even at a moderate frictional force. It follows that stress concentration in the contact area enhance the abrasion process for similar external forces [1].

CHAPTER 3 : RESULTS

3.1 FRICTIONAL FORCE

Frictional force acting on bodies in contact with ground is given by using general formula

$$F_{\text{frictional}} = \mu * N$$

Where,

μ is coefficient of friction between ground and the body

N is Normal load or weight of the body

We need to find normal load and coefficient of friction to get frictional force

3.2 NORMAL LOAD DISTRIBUTION

Images obtained using FTIR technique was used to find load distribution. Matlab was used as tool for image processing. Results obtained are discussed below.

Images obtained from FTIR technique were imported in Matlab. These images were converted to gray scale for ease of operation. Any pixel not representing tire footprint, i.e noise was filtered out for accurate results. As discussed earlier load distribution across footprint is proportional to light intensity in images obtained in FTIR, a constant of proportionality was calculated. Each pixel in the images array was multiplied by the constant of proportionality. Now each element in the image array represents vertical load at corresponding pixel. This array was plotted as a load distribution surface plot. This

load distribution data was curve fitted using 4th order polynomial and plotted with better resolution.

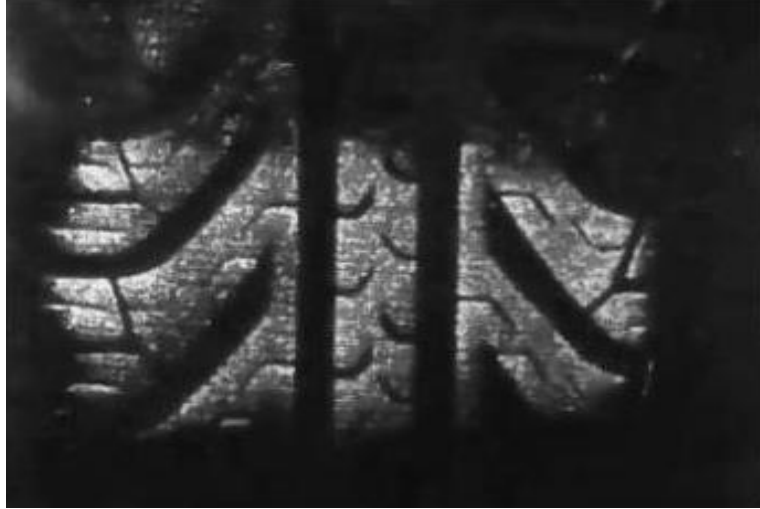


Figure 26: Gray scale footprint for 0° camber



Figure 27: gray scale footprint for 0° camber after deleting noise

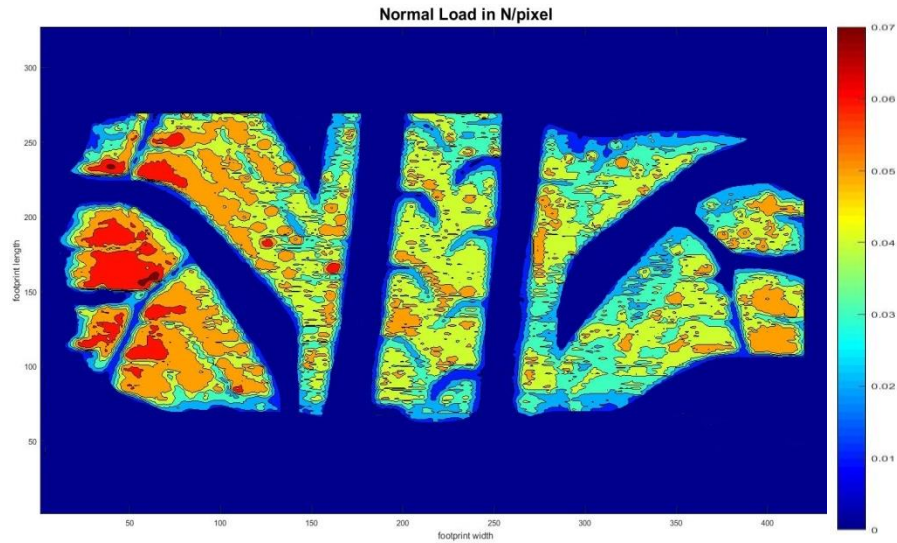


Figure 28: tire footprint and load distribution in tire contact patch for 6° slip angle

The darker red colored contour gradient on the inner shoulder element indicates a higher pressure. We can notice from pressure distribution images that as camber increase in positive direction, pressure on outer shoulder also increases. Pressure is higher on leading edge of tire.

3.3 COEFFICIENT OF FRICTION

Peter Tkacik [15] presented the relationship between coefficient of friction and rubber properties G' , $\tan\delta$, normal stress. Using his work as a reference coefficient of friction was obtained.

$$\mu = 0.262200 * G' * \tan(\delta) / (\sigma_n)^{0.826097}$$

where,

G' - Shear modulus of elasticity

σ_n – Normal stress

Using footprints obtained with FTIR technique, coefficient of friction is obtained for each pixel individually. The distribution of coefficient of friction at contact patch is shown in figure 29. As μ is inversely proportional to normal stress we can observe that μ is low in areas where normal load distribution is higher. Frictional force or shear force due to friction is obtained from normal load distribution and coefficient of friction.

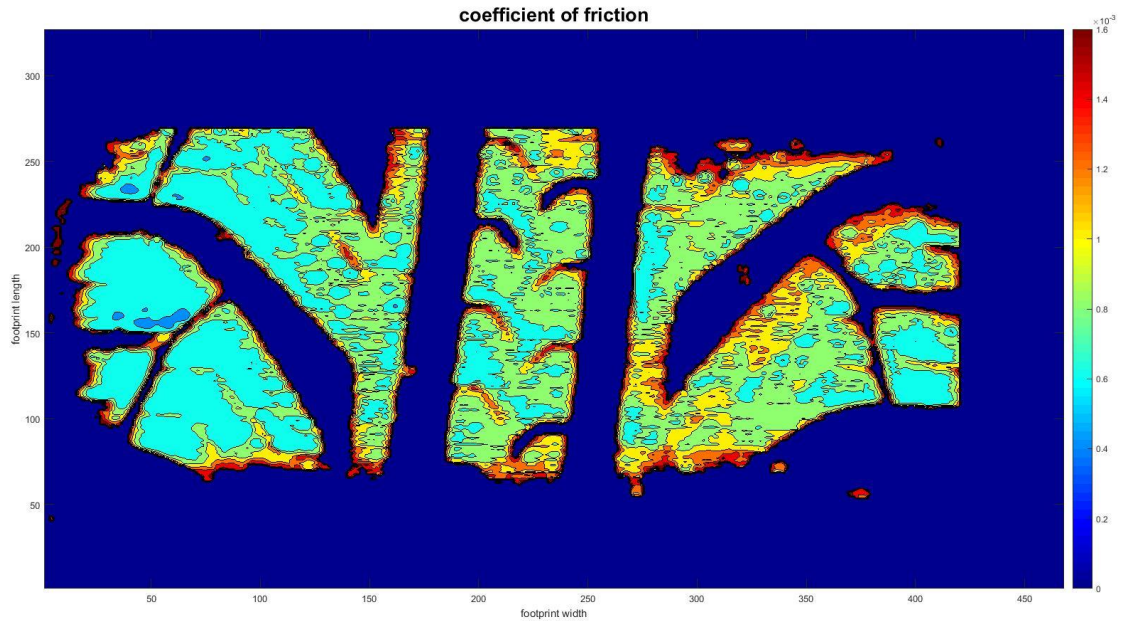


Figure 295: Coefficient of friction across contact patch

Frictional force is calculated from product of matrices coefficient of friction and normal load. The distribution is plotted on contact patch

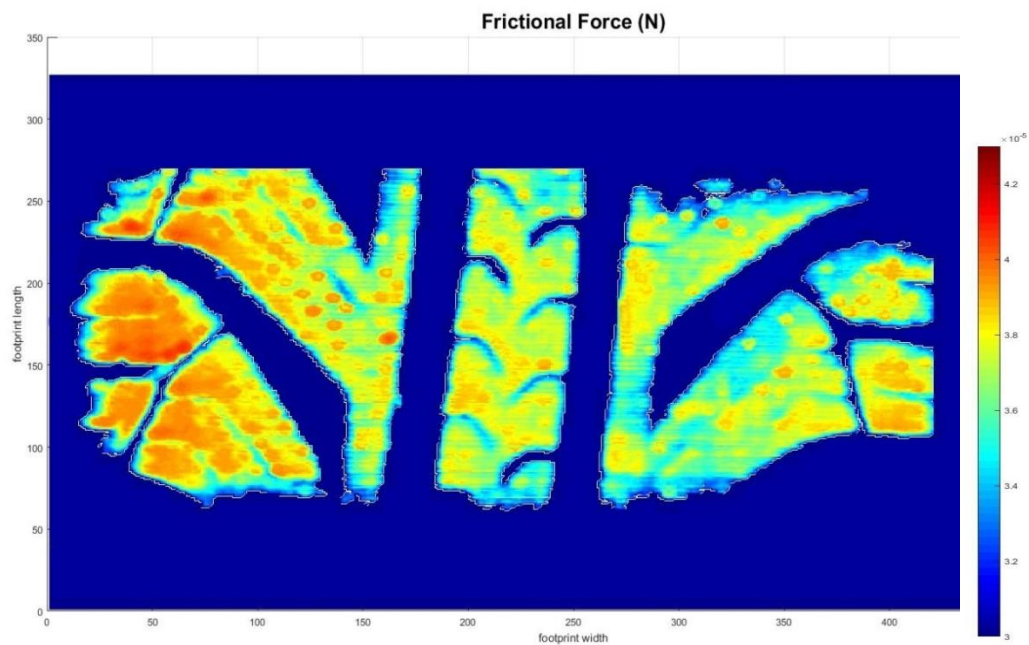


Figure 26: Frictional force distribution at contact patch for 6 degree slip angle

3.4 TREAD DISPLACEMENT

Technique of Total Internal Reflection was used instead of FTIR to find tread displacement. The difference in two methods is FTIR uses a sheet to frustrate total internal reflection which helps determining load intensity. Methodology used for strain energy distribution is described below. As discussed earlier strain energy is energy stored in solid while undergoing deformation. Finding tread block deformation during rolling is relatively harder. White spray paint was sprinkled on tire surface so that small white paint dots can be tracked while rolling tire in contact with road surface, in this case glass surface. Tire rolling on glass with total internal reflection setup to glow footprint was shot with 30 frames per second video. Dentec Dynamic Studio; a PIV (Particle Image Velocitrometry) software capable of tracking moving particles was used to track movement of spray painted dots on the tire footprint between two consecutive frames. Dynamics studio compares consecutive frames for position of particles. Measurement was done at 2.3 degree camber angle.



Figure30: Tire with paint for displacement measurement



Figure 31: Tire footprint with sprayed paint at 6° slip angle

Dentec Dynamic studio was fed with multiple frames of paint sprayed tire footprint video. Lateral and longitudinal velocity vectors of each individual dot were obtained. But there are some limitations of the software and it tends to track particles not on a contact patch as well dust particles. Such a noise has to be filtered. Particles with velocity vectors greater than 2mm/sec were not considered for the calculations. Any particle lying outside footprint travel path was also disregarded.

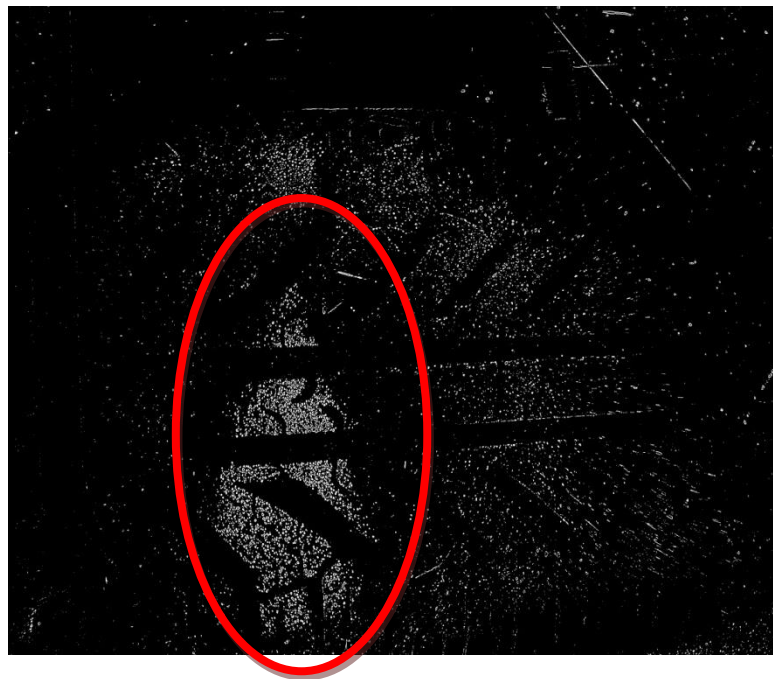


Figure 32: All the particles tracked by dynamic studio red circle shows contact patch at 2.3° camber angle

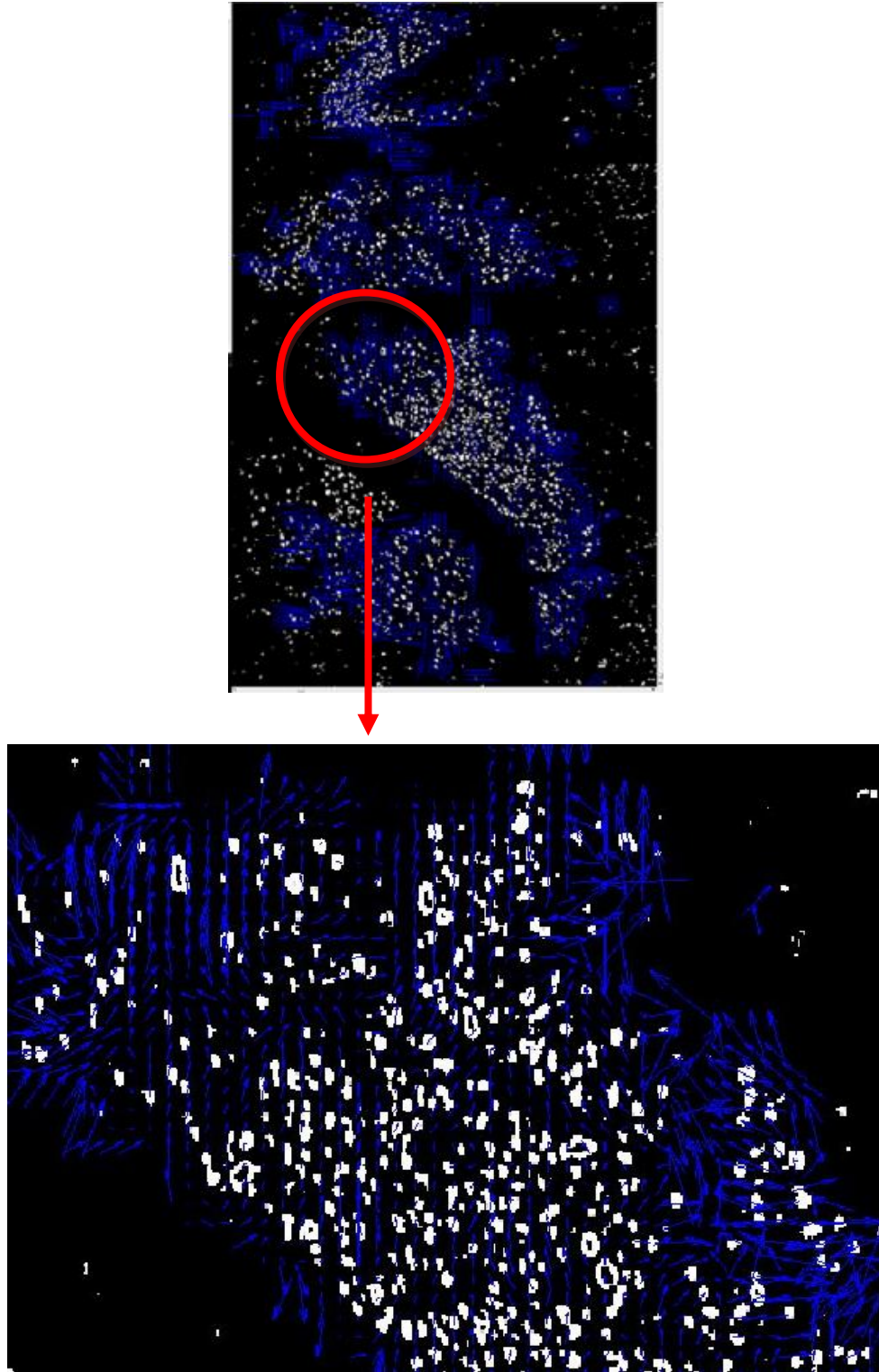


Figure 33: 90⁰ rotated view and zoomed view of velocity vectors of points on contact patch

3.5 SHEAR ENERGY INTENSITY

Figure shows velocity vectors velocity vectors of particles on contact patch after neglecting noise. Velocity at contact patch edge is more than that at center. The software gives both lateral and longitudinal velocities of points and their co-ordinates. The excel sheet containing all the velocity data was imported in matlab. All velocity vectors were stored in matrix as a function of contact patch length and width. Velocities were curve fitted using 2nd order polynomial for better resolution across contact patch. As we know time gap between consecutive frames, displacement of particles can be calculated.

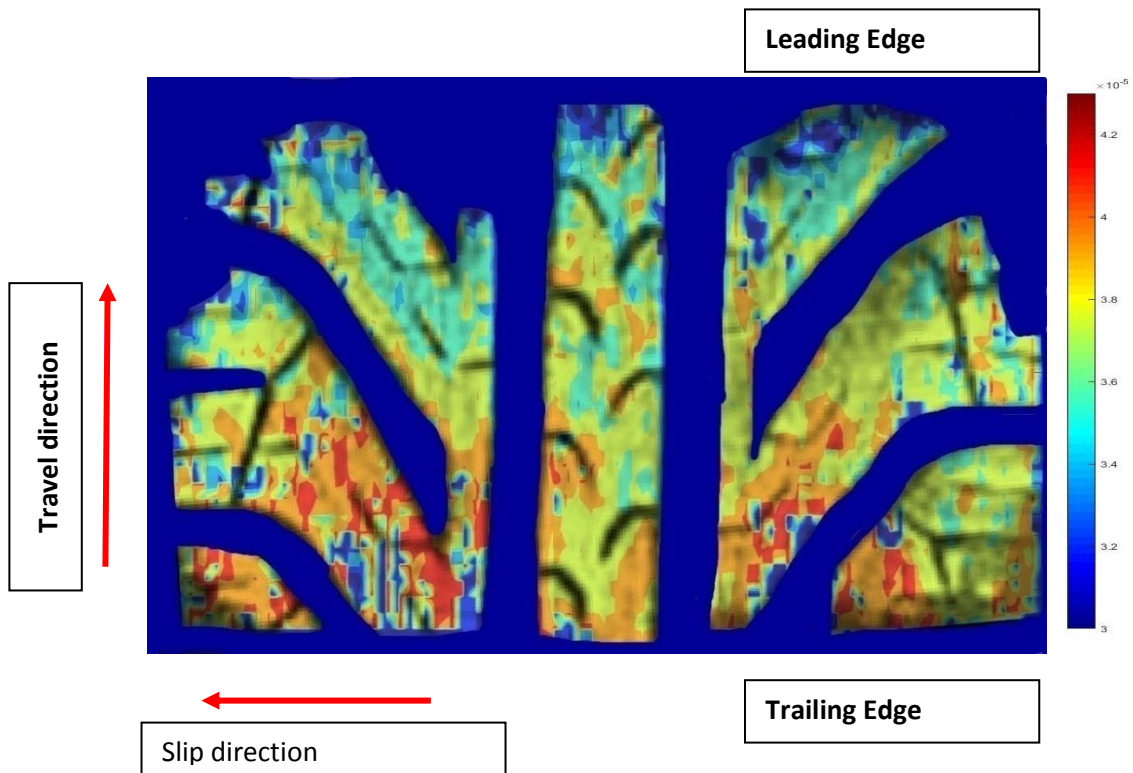


Figure 34: displacement contour across contact patch for 6 degree slip angle in mm

Shear energy intensity is obtained using formula discussed in earlier section. Shear energy is plotted across contact patch.

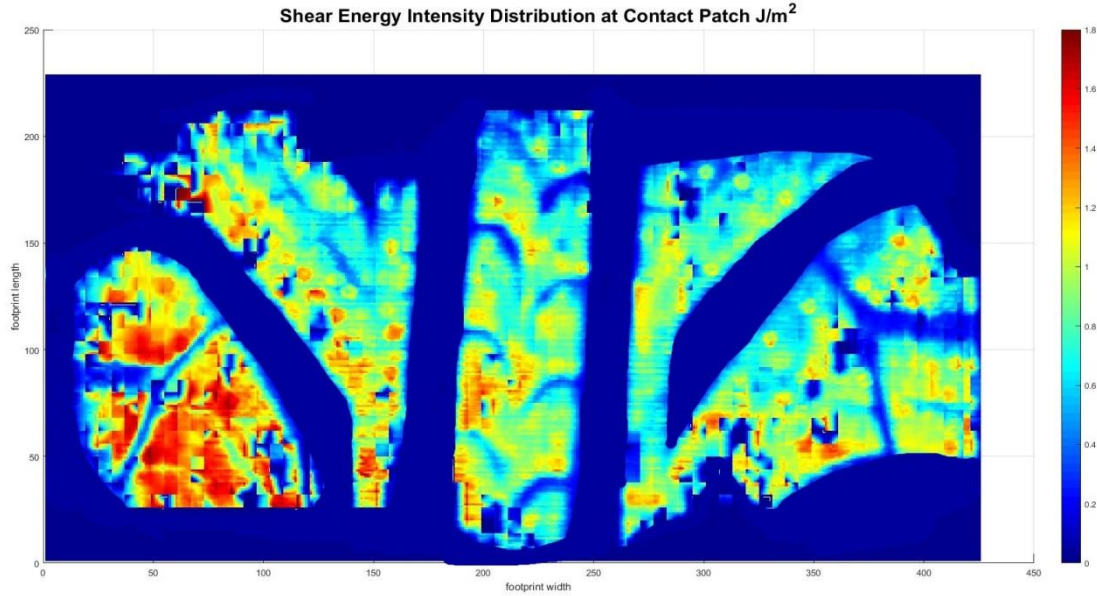


Figure 35: Shear Stress Intensity across contact patch at 6 degree slip angles

We can see from shear energy distribution contour that shear energy magnitude is highest at trailing edge of sliding tire. Further, magnitude of shear energy at trailing in a direction of slip angle is more than that of other end. Shear energy intensity on leading edge of tire is lowest.

CHAPTER 4: CONCLUSION

A method to obtain contact pressure distribution in tire footprint was developed using concept frustrated total internal reflection. The method was developed with tires mounted on vehicle as well as tires in rolling motion. Images obtained were pretty satisfactory and logical suggesting the method yields correct results. Pressure distribution was found using image processing tools. The optical approach is faster and cheaper way to find the shear energy intensity.

A method to measure tread displacement of rolling tire under load was developed. A method to combine load distribution and tread displacement was successfully developed. Shear energy i.e energy dissipated due to frictional force or shear stress at contact patch was obtained using the developed method. Studying shear energy at different suspension settings will help to understand tendency of tire wears. Shear energy intensity distribution at contact patch can also be compared with tire wear. The relationship between shear energy and tire wear can help better understand phenomenon of tire wear.

Effect of varying camber angles on contact pressure distribution was studied. It could be seen that as camber angle increases, normal pressure at contact on edge with inclination also increases. It suggests more grip can be achieved with increasing camber angle. However increasing camber above some limit reduces overall tire contact patch width. Uneven load distribution in contact patch at higher camber angles will also cause irregular wear in tire. More wear can be seen at side/shoulder in a direction tire inclination.

CHAPTER 5 FUTURE SCOPE

FTIR concept was used to find contact patch pressure/load distribution. This technique can be further improved with more control on ambient conditions for better picture quality.

PIV software dynamics studio can accurately predict particle displacement. But It has some drawbacks. The software sometimes gets confused if particles from previous frame are absent in the next frame. It may show very high displacement values or zero displacement. Tread deformation accuracy can be improved by solving this issue.

Study shear energy in contact patch at various slip angles, inclination angles to find effect of inclination, slip, pressure on shear energy intensity in contact patch.

Establishing relationship between shear energy intensity in contact patch and tire wear will be next major step to understand effect of shear energy intensity on tire wear.

BIBLIOGRAPHY

1. N.Gent, J.D.Walter, "The pneumatic Tire," National Highway Traffic Safety Administration U. S. Department of Transportation, DOT Contract DTNH22-02-P-07210
2. <https://www.rqriley.com/suspensn.htm/>
3. G. Heinrich , M. Klueppel, "Rubber friction, tread deformation and tire traction," Wear 265(7):1052-1060 , September 2008
4. <http://wiygul.com/support/1386/how-to-tell-if-your-vehicle-needs-an-alignment/>
5. Yeong-Jyh Lin, Sheng-Jye Hwang, "Temperature prediction of rolling tires by computer simulation, Mathematics and Computers in Simulation" 67 (2004) 235–249 ,Published by Elsevier B.V.
6. D. A. van den Ende, H. J. van de Wiel, W. A. Groen and S. van der Zwaag, "Direct strain energy harvesting in automobile tires using piezoelectric PZT–polymer composites," Smart Materials and Structures, Volume 21, Number 1
7. Y. Xiong, A. Tuononen, "optical measurement of tread deformation for rolling resistance studies," The 23rd International Symposium on Dynamics of Vehicles on Roads, Qingdao, China, August 19-23, 2013. Qingdao,China
8. C. R. Gentle, "Optical Mapping of Pressures in Tire Contact Areas," Opt. Lasers Eng.1983, 4, 167–176
9. J.Castillo, A.Perez De La blanca, J. A. Cabrera, A.Simon, "An optical tire contact pressure test bench,"Vehicle System Dynamics 44(3):207-221 · March 2006

10. S.Knisley, “ A Correlation Between Rolling Tire Contact Friction Energy and Indoor Tread Wear,” Tire Science and Technology, TSTCA, Vol. 30, No. ,April-June 2002, pp. 83-99
11. M. G. Pottinger, J. E. McIntire, “Effect of Suspension Alignment and Modest Cornering on the Footprint Behavior of Performance Tires and Heavy Duty Radial Tires,” Tire Science and Technology, TSTCA, Vol. 27, No. 3, July-September 1999, pp. 128-160.
12. J .S Dick, “Basic Rubber Testing: Selecting methods for rubber test program,” ASTM stock number MNL39
13. J. Y. Wong, “Theory of Ground Vehicles,” John Wiley & Sons, Mar 20, 2001
- 14.J. Yunta, O. Olatunbosun, X. Yang, V. Diaz, “A Strain-Based Method to Estimate Slip Angle and Tire Working Conditions for Intelligent Tires Using Fuzzy Logic”, , *Sensors* 2017, 17(4), 874; doi:10.3390/s17040874
15. P. Tkacik, “ A hybrid Model using Finite Element Method and Machine Vision to Study Contact Problem’, Phd desertation, submitted in University of South Carolina, 1991
16. <http://www.dexel.co.uk/services/alignment/>